Astron. Astrophys. 324, L77–L80 (1997)

ASTRONOMY AND ASTROPHYSICS

LETTER

Letter to the Editor

Soft X-ray observations of the complex warm absorber in MCG-6-30-15 with BeppoSAX

Astrid Orr[1], **S. Molendi**[2], **F. Fiore**[3], **P. Grandi**[4], **A.N. Parmar**[1], **and Alan Owens**[1]

[1] Astrophysics Division, Space Science Department of ESA, ESTEC, P.O. Box 299, 2200 AG Noordwijk, The Netherlands
[2] Instituto di Fisica Cosmica e Tecnologie Relative C.N.R., Via Bassini 15, I-20133 Milano, Italy
[3] BeppoSAX Science Data Center, c/o Nuova Telespazio, Via Corcolle 19, I-00131 Roma, Italy
[4] Instituto di Astrofisica Spaziale C.N.R., Via Enrico Fermi 21-23, I-00044 Frascati, Italy

Received 13 May 1997 / Accepted 10 June 1997

Abstract. We report on soft X-ray observations of the Seyfert 1 galaxy MCG-6-30-15 with the Low and Medium Energy Concentrator Spectrometers on board BeppoSAX. The time averaged 0.1–4 keV spectrum shows evidence for a complex warm absorber. K-edges of highly ionized oxygen (O VII and O VIII) can only partly describe the soft X-ray spectrum below 2 keV. A spectral variability study reveales large and rapid changes in absorption at the energy of the O VIII K-edge and in the continuum shape and count rate. These fluctuations are not simply correlated.

Key words: Galaxies: individual: (MCG-6-30-15) – Galaxies: Seyfert – X-rays: galaxies

1. Introduction

The well studied and nearby (z = 0.008) Seyfert 1 galaxy MCG-6-30-15 displays complex X-ray emission. Strong and rapid variability, as well as intrinsic absorption and possibly a "soft excess" component were first detected with EXOSAT (Pounds et al. 1986). MCG-6-30-15 was among the first objects in which a spectral "hump" was observed above 10 keV (Pounds et al. 1990) suggesting the reprocessing of hard X-rays by cold, optically thick reflecting matter. The ROSAT Position Sensitive Proportional Counter (PSPC; Nandra & Pounds 1992) provided evidence for the presence of highly ionized "warm" absorbing medium close to the X-ray continuum source. This absorption was detected as a feature at 0.8 keV, consistent with a blend of O VII and O VIII K-edges. ASCA performed further observations of MCG-6-30-15 (Fabian et al. 1994; Reynolds et al. 1995; Otani et al. 1996), which indicate short term variability of the warm absorber. Reynolds et al. (1995) and Otani et al. (1996) report dissimilar variability patterns in the depth of the O VII and O VIII K-edges and conclude that these features must originate at different distances from the central engine.

Send offprint requests to: A. Orr: aorr@astro.estec.esa.nl

2. Observations

MCG-6-30-15 was observed by the BeppoSAX satellite as part of the Science Verification Phase between 1996 July 29, 15:56 and August 03, 03:15 UT. The data reported here were obtained using the Low and Medium Energy Concentrator Spectrometers (LECS & MECS). The LECS and MECS are position sensitive gas scintillation proportional counters, sensitive in the energy range 0.1–10 keV and 1.3–10 keV respectively with circular fields of view of diameters 37' and 56' (LECS: Parmar et al. 1997; MECS: Boella et al. 1997). The LECS has good spectral resolution at energies $\lesssim$ 0.5 keV, where instruments such as the Solid State Imaging Spectrometer (SIS) on ASCA are not sensitive (see Tanaka et al. 1994) and where instruments such as the ROSAT PSPC (0.1–2.5 keV; Trümper 1983) have only moderate spectral resolution. Above 1.8 keV the effective area of the MECS is larger than that of the LECS. The total on-source exposure is 49.4 ksec for the LECS and 184 ksec for the MECS. Data from the LECS and the MECS were prepared in a similar way (the MECS data are discussed in further detail by Molendi et al. 1997). gas Imaging LECS data were processed using the SAXLEDAS 1.4.0 data analysis package (Lammers 1997). The mean spectrum was extracted within a radius of 4′ of the source centroid, corresponding to 55 % of the encircled energy at 0.28 keV in the LECS. Light curves and the spectra for several shorter time intervals were obtained using an 8′ LECS extraction radius which includes 95% of the 0.28 keV photons. Background subtraction was performed using a 46 ksec exposure obtained by summing blank field observations at galactic latitudes close to that of MCG-6-30-15 ($\Delta b < 5.3°$). After

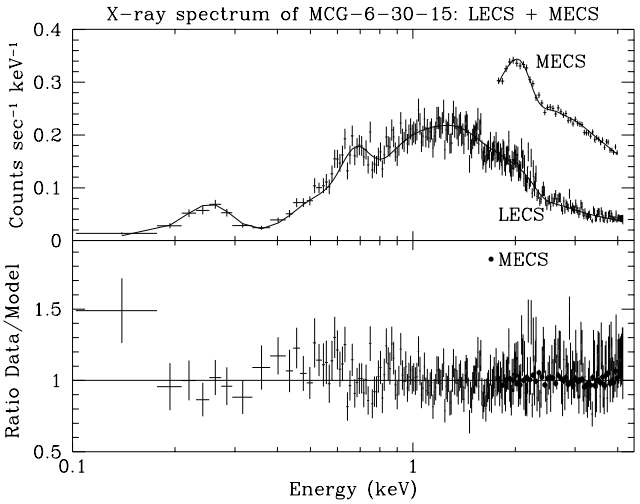

Fig. 1. The combined LECS/MECS X-ray spectrum of MCG-6-30-15. The 1.8–4 keV data set is from the MECS. Top panel, observed mean 0.1–4 keV spectrum fitted by a power-law, an absorption edge and galactic plus excess neutral absorption (model 2 of Table 1). Lower panel, ratio of data and model. The residuals are discussed in the text

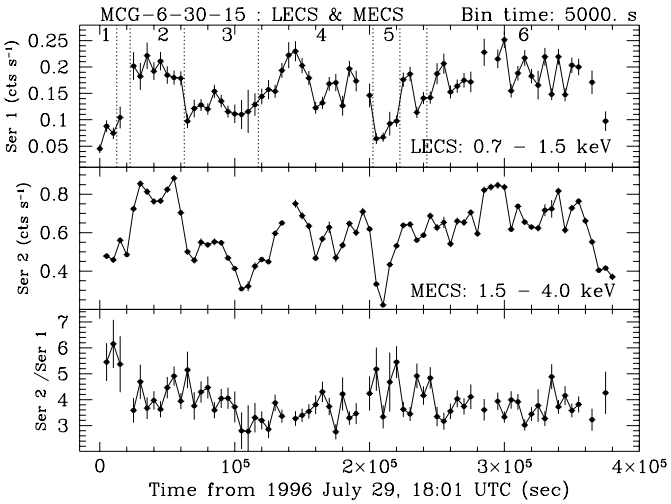

Fig. 2. Top: 0.7–1.5 keV LECS light curve of MCG-6-30-15 within a radius of 8′ of the source centroid. The epochs chosen for the study of spectral variability are numbered from 1 to 6. Middle: 1.5–4.0 keV MECS light curve (4′ radius). Bottom: ratio of 1.5–4.0 keV counts over 0.7–1.5 keV counts. The corresponding background count rates are negligible; LECS: $(5.40 \pm 0.38)\,10^{-3}\,\mathrm{s}^{-1}$; MECS: $(1.45 \pm 0.13)\,10^{-3}\,\mathrm{s}^{-1}$

background subtraction and with a 4 ′ extraction radius, the LECS count rate is 0.5243 ± 0.0033 s^{-1} and that of the MECS is 1.0370 ± 0.0025 s^{-1}.

3. Spectral fits

Fits to LECS and MECS data were performed in order to describe the mean spectrum of MCG-6-30-15, as well as to investigate possible spectral variability between selected time intervals. Fe Kα emission contributes significantly to the flux between 4–10 keV (Tanaka et al. 1995; Iwasawa et al. 1996; Molendi et al. 1997). Therefore data above 4 keV are not considered for the present study which focuses on the soft X-ray range, but are discussed by Molendi et al. (1997). The simultaneous fitting of LECS and MECS observations imposes strong constraints on the spectral energy distribution in the common energy range from 1.8–4.0 keV while benefiting from the good spectral resolution of the LECS at lower energies. All fit models include a constant multiplicative factor to account for the LECS/MECS inter-calibration. This factor varied no more than 2% between the different models fitted.

A minimum of at least 20 source counts per spectral bin was chosen to ensure meaningful χ^2 values. Uncertainties correspond to $\Delta\chi^2 + 2.706$, unless otherwise stated.

3.1. The mean spectrum

Table 1 describes the various fits to the mean 0.1 to 4 keV spectrum of MCG-6-30-15. A simple power-law fit with photo-electric absorption fixed at the galactic hydrogen column density $N_{Gal} = 4.06 \times 10^{20}$ cm^{-2} (Elvis et al. 1989) gives a poor fit (χ^2 = 707.1 with 400 degrees of freedom, dof) with large residuals below 2 keV.

Including excess photo-electric absorption and an absorption edge component to account for a blend of O VII and O VIII gives a significantly better fit (χ^2 =418.4 with 396 dof; Fig. 1). Allowing for excess absorption improves the quality of the fit in all models considered. This was also the case for ASCA observations (Otani et al. 1996).

560

We have tried to fit the warm absorber in the LECS mean spectrum with two absorption edges. However the fits do not require two separate edges around the physical rest frame energies of the O VII and O VIII K-edges: 0.74 and 0.87 keV. This is most likely due to a combination of effects, such as the temporal variability of the optical depths of the edges (reported by Fabian et al. 1994, Reynolds et al. 1995 and Otani et al. 1996) which can bias the energy of the O VII and O VIII edge blend. Also, the energy resolution of the LECS in this energy range is poorer than that of the SIS on ASCA. Little improvement in fit quality is obtained with two edges fixed at these energies (χ^2 = 415.9 with 396 dof).

The fit residuals for all models mentioned above show complex structure below 1 keV. Otani et al. (1996) included an *ad hoc* Gaussian emission line at 0.6 keV to improve their fits to the mean ASCA spectrum. A Gaussian line also provides a better fit to the LECS mean spectrum (E_{rest} = 0.59 $\pm$ 0.03 keV; EW = 44.5 ± 30.7 eV; χ^2 = 403.8 with 394 dof). The energy of the line is consistent with a blend of O VII and O VIII recombination lines at E_{rest} = 0.57 and 0.65 keV, respectively, which are unresolved by the LECS. The resulting reduction of χ^2 is significant at the 99% level on the basis of an F-test. The line is narrower than the resolution of the LECS (which is 140 eV at 0.6 keV) and when left as a free fit parameter the line width, σ,

Table 1. Results of combined LECS/MECS fits to the mean 0.1 to 4 keV spectrum of MCG-6-30-15. All fits include photo-electric absorption with $N_{Gal} = 4.06 \times 10^{20}$ cm^{-2}. The uncertainties are $\Delta\chi^2 + 2.706$. Rest frame energies are given for the quoted absorption edges and emission lines. Parameters without uncertainty values were fixed during the fitting

	model	excess N_H (10^{20} cm^{-2})	photon index Γ	E_{edge} (keV)	τ_{edge}	E_{line} (keV)	χ^2/d.o.f
1	PL	...	1.68 ± 0.01	...	...	...	707.1/400
2	PL+edge	1.86 ± 0.30	1.89 ± 0.02	0.77 ± 0.02	0.81 ± 0.10	...	418.4/396
3	PL+2 edges	1.94 ± 0.31	1.90 ± 0.02	0.74 0.87	0.65 ± 0.14 0.22 ± 0.11	...	415.9/396
4	PL+2 edges + line	1.89 ± 0.33	1.88 ± 0.03	0.74 0.87	0.66 ± 0.14 0.14 ± 0.12	0.59 ± 0.03	403.8/394
5	PL+3 edges	2.36 ± 0.38	1.95 ± 0.03	0.74 0.87 1.12 ± 0.10	$0.91 \pm {}^{0.18}_{0.14}$ 0.03 ± 0.15 0.19 ± 0.08	...	398.1/394

becomes zero. Consequently the line width has been fixed at 10 eV.

The parameters of the warm absorber component and in particular the optical depths depend on the shape of the underlying continuum. As can be seen in Table 1 the power-law index remains almost constant for models 2 to 4, since it essentially constrained by the data above 1 keV. However, this spectral range may not be representative of the underlying continuum flux. In particular a blend of absorption edges may considerably affect the spectral range up to 3 keV (Ferland 1996; Nicastro et al. in preparation), thereby causing the local spectrum to be harder than the underlying continuum. In order to test this hypothesis we have added a Ne IX absorption edge to the fit (model no. 5 in Table 1). Its energy is $E_{rest} = 1.12 \pm 0.10$ keV which is compatible with the physical value of 1.20 keV. The decrease in χ^2 with respect to model no. 3 including only oxygen edges is significant at the 99% level on the basis of an F-test. Furthermore the photon index in model 5 is marginally steeper than with models 2 – 4, as expected.

In conclusion, none of the models described above gives an entirely satisfactory fit to the mean 0.1–4 keV spectrum of MCG-6-30-15, although the addition of various components discussed can significantly reduce χ^2. In particular, residual flux remains below 0.2 keV. Features below the C-edge (0.28 keV) are very sensitive to the subtracted background which has a soft component in this spectral range (Hasinger et al. 1993). Furthermore the diffuse soft X-ray background map obtained with the ROSAT PSPC (Snowden et al. 1995) shows considerable structure. For all these reasons background subtraction is complex. We have deliberately chosen a small extraction radius for the LECS spectra in order to reduce the contributions from the background.

3.2. Spectral variability

Because of the difficulty in obtaining satisfactory fits to the mean spectrum, we have investigated whether this is due to spectral variability. The LECS 0.7–1.5 and MECS 1.5–4.0 keV light curves of MCG-6-30-15, as well as their ratio, are shown in Fig. 2. As seen in the previous section, warm absorption strongly affects the first spectral range, but much less the second. Flux variations of the order of a factor 4 occured during our observation. In fact, at the start of the observation the 0.7–1.5 keV count rate increased four-fold in <7 hours while the 0.7–4 keV spectrum was in a "hard" state. Such behaviour suggests a change in the warm absorber. We performed time resolved spectral analysis in order to check which ion species (O VII or O VIII) had varied. For ease of analysis we selected six "low" and "high" states, with average LECS 0.1–10 keV count rates respectively below or above a value of 0.5 cts s^{-1}. This choice is by definition inhomogeneous, because of complex time structure within the time intervals. In particular, some data between intervals have been excluded.

Model 3 is used to fit the time selected LECS+MECS spectra from 0.1–4 keV. Figure 3 shows that the optical depths $\tau_{\rm OVII}$ and $\tau_{\rm OVIII}$ have different variability patterns. The depth of the O VII edge is marginally consistent with being constant throughout the LECS observation, whereas $\tau_{\rm OVIII}$ exhibits significant variability. Its large value during interval 1 (1.7 ± 0.5, 1σ uncertainty) is inconsistent with the values at all other epochs, and is the cause of the spectral hardening at epoch 1 (Fig. 2, lower panel). Epoch 1 stands out as having a more extreme value of $\tau_{\rm OVIII}$ and count rate variability than observed by ASCA in 1993 and 1994 (Fabian et al. 1994; Reynolds et al. 1995; Otani et al. 1996). This epoch is characterized by a very rapid increase in count rate. Since the source count rate prior to our observation is unknown, the ionizing flux could have been much lower earlier, leading to the high value of $\tau_{\rm OVIII}$ observed.

4. Discussion

Our results indicate that the spectral variability of MCG-6-30-15 from 0.1–4 keV is due to changes in the continuum emission as well as modifications of the warm absorber. These variations

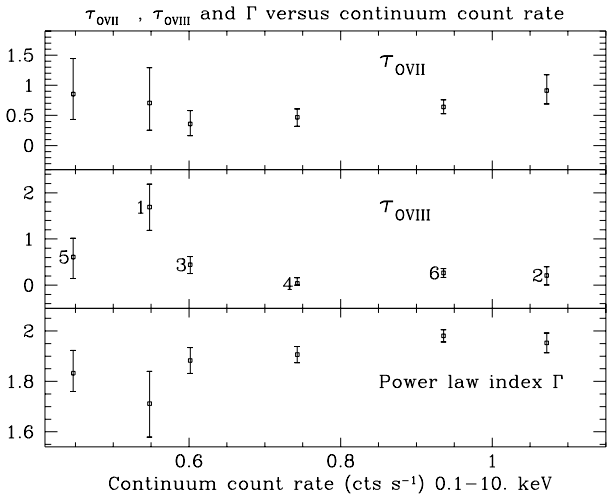

Fig. 3. Photon index, Γ, $\tau_{\rm OVII}$ and $\tau_{\rm OVIII}$ versus un-absorbed model continuum count rate from 0.1 to 10 keV. The 0.1–4 keV fits use model 3 of Table 1. Uncertainties are $\Delta\chi^2$ + 1.0. In the middle panel, each point is identified by its epoch number as defined in Fig. 2

have similar timescales, but are not always associated with one another. For instance during epoch 5 (Figs. 2 and 3) the 1.5–4 keV flux undergoes a rapid ($\tau_{var} < 2\times10^4$ s) decrease followed by an equally fast increase. With such rapid changes it is possible that the absorber is not in photo-ionization equilibrium. Indeed, the spectrum of epoch 5 shows no evidence of change in the warm absorber.

Likewise, the spectral softening before high state 6 is not accompanied by any significant change in $\tau_{\rm OVII}$ or $\tau_{\rm OVIII}$. Spectral softening with increasing flux was also observed in MCG-6-30-15 by Ginga in the 2–18 keV band and variously interpreted by several groups (Matsuoka et al. 1990; Nandra et al. 1990; Fiore et al. 1992). A more detailed analysis of these variations in the BeppoSAX data is presented by Molendi et al. (1997).

There are clear indications that more than one absorption edge is present below 1 keV. Models including both an O VII and an O VIII absorption edge bring little improvement to the quality of fit over single edge models. However, single edge models are physically unacceptable because the spectral fits to the time intervals then require temporal variations of the edge energy. The LECS data show that the optical depth $\tau_{\rm OVII}$ did not change significantly during the exposure, whereas $\tau_{\rm OVIII}$ varied on a time scale $\leq$ 15 000 seconds (epochs 1 & 2 in Figs. 2 and 3). Differences between $\tau_{\rm OVII}$ and $\tau_{\rm OVIII}$ have been reported by Reynolds et al. (1995) and Otani et al. (1996). However, unlike what was measured with ASCA, our data show no simple anti-correlation between $\tau_{\rm OVIII}$ and the continuum luminosity. A warm absorber consisting of spatially distinct photo-ionized regions, such as the two-zone model applied to ASCA data (Reynolds et al. 1995; Otani et al. 1996), does not provide an entirely satisfactory explanation to such behaviour. A plausible interpretation is that the warm absorber is not in simple photo-ionization equilibrium with the incident X-ray continuum. More complex processes, such as non-equilibrium – or collisional photo-ionization, may instead contribute to the soft X-ray spectrum of MCG-6-30-15.

Acknowledgements. The authors wish to thank the BeppoSAX science team members. The BeppoSAX satellite is a joint Italian and Dutch programme. Astrid Orr acknowledges an ESA Research Fellowship.

References

Boella G., Chiappetti L., Conti G., et al., 1997, A&AS 122, 327
Elvis M., Lockman F., Wilkes B., 1989, AJ 97, 777
Fabian A., Kunieda H., Inoue S., et al., 1994, PASJ 46, L59
Ferland G., 1996, CLOUDY:90.01
Fiore F., Perola G., Matsuoka M., Yamauchi M., Piro L., 1992, A&A 262, 37
Hasinger G., Burg R., Giacconi R., et al., 1993, A&A 275, 1
Iwasawa K., Fabian A., Reynolds C., et al., 1996, MNRAS 282, 1038
Lammers U., 1997, The SAX LECS Data Analysis System, 1997, Internal Report ESTEC SAX/LEDA/0010, ESA
Matsuoka M., Piro L., Yamauchi M., Murakami T., 1990, ApJ 361, 440
Molendi S., et al., in preparation
Nandra K., Pounds K., Stewart G., 1990, MNRAS 242, 660
Nandra K., Pounds K., 1992, Nature 359, 215
Nicastro F., Fiore F., Perola C., Elvis M., in preparation
Otani C., Kii T., Reynolds C., et al., 1996, PASJ 48, 211
Parmar A., Martin D., Bavdaz M., et al., 1997, A&AS 122, 309
Pounds K., Turner T., Warwick R., 1986, MNRAS 221, 7p
Pounds K., Nandra K., Stewart G., George I., Fabian A., 1990, Nature 344, 132
Reynolds C., Fabian A., Nandra K., et al., 1995, MNRAS 277, 901
Snowden S., Freyberg M., Plucinsky P., et al., 1995, ApJ 454, 643
Tanaka Y., Inoue H., Holt S.S., 1994, PASJ 46, L37
Tanaka Y., Nandra K., Fabian A., et al., 1995, Nature 375, 659
Trümper J., 1983, Adv. Space Res. 2, 241

This article was processed by the author using Springer-Verlag LaTeX A&A style file *L-AA* version 3.